2
Molecular Metal Oxides and Clusters as Building Blocks for Functional Nanoscale Architectures and Potential Nanosystems

Leroy Cronin

2.1
Introduction

Lithography has enabled the miniaturization revolution in modern technology, with over 800 million transistors being packed into the latest multicore processor architectures. Despite these great advances in technology, the ability of top-down approaches to access smaller and smaller architectures is limited. Therefore, the use of chemical self-assembly from molecular building blocks holds great promise to enable fabrication on the nanoscale, or even the sub-nanoscale. By controlling molecular organization it will be possible to develop functional nano-systems and nanomachines, ultra-high-capacity information storage materials [1], molecular electronics [2], and sensors [3]. However, there are many fundamental issues that need to be tackled, including the design of systems that can be synthe-sized or self-assembled in a predetermined manner to form highly complex architectures.

Here we are going to discuss a class of molecules and materials that have nanoscale architectures that can be controlled and begin to suggest how these building blocks may eventually be used for the fabrication of nanoscale devices. These building blocks are based upon a class of inorganic clusters known as poly-oxometalates (POMs), and appear to have a great many desirable characteristics applicable for nanoscale assembly. This is because nanoscale polyoxometalate clusters provide an arguably unrivaled structural diversity of molecules displaying a wide range of important physical properties and nuclearities; these cover the range from 6 to 368 metal ions in a single molecule and are assembled under "one-pot" reaction conditions [4]. At the extreme, these cluster molecules are truly macromolecular, rivaling the size of proteins, and are formed by self-assembly processes [5].

The POM clusters tend to be anionic in nature, being based upon metal oxide building blocks with a general formula of MO_x, (where M is Mo, W, V and sometimes Nb and x can be 4, 5, 6 or 7). POM-based materials have a large range of interesting physical properties [6–10] which result from their many structures, the ability to delocalize electrons over the surface of the clusters, and the ability

to incorporate heteroanions, electrophiles, and ligands, and to encapsulate guest molecules within a the metal-oxo cage defined by the POM. Further, POM clusters have been shown to exhibit superacidity [6], catalytic activity [6], photochemical activity [7], ionic conductivity [7], reversible redox behavior [8], bistability [7], cooperative electronic phenomena [7], the ability to stabilize highly reactive species [9], and extensive host–guest chemistry [10].

The large number of structural types in polyoxometalate chemistry [11] can be broadly split into three classes. (i) Heteropolyanions: these are metal oxide clusters that include heteroanions such as SO_4^{2-}, PO_4^{3-}. These represent by far the most explored subset of POM clusters, with over 5000 papers being reported on these compounds during the last four years alone. Much of this research has examined the catalytic properties of POMs with great emphasis on the Keggin $\{XM_{12}O_{40}\}$ and the Wells–Dawson $\{X_2M_{18}O_{62}\}$ (where M = W or Mo and X = a tetrahedral template) anions which represent the archetypal systems. In particular W-based POMs are robust and this has been exploited to develop W-based Keggin ions with vacancies that can be systematically linked using electrophiles to larger aggregates [4, 11]. (ii) Isopolyanions: these are composed of a metal-oxide framework, but without the internal heteroatom/heteroanion. As a result, they are often much more unstable than their heteropolyanion counterparts [12]. However they also have interesting physical properties such as high charges and strongly basic oxygen surfaces, which means they are attractive units for use as building blocks [13]. (iii) Mo-blue and Mo-brown reduced POM clusters: these are related to molybdenum blue type species, which were first reported by Scheele in 1783 [14]. Their composition was largely unknown until Müller *et al.* reported, in 1995, the synthesis and structural characterization of a very high-nuclearity cluster $\{Mo_{154}\}$ crystallized from a solution of Mo-blue, which has a ring topology [15]. Changing the pH and increasing the amount of reducing agent along with incorporation of a ligand like acetate facilitates the formation of a $\{Mo_{132}\}$ spherical ball-like cluster [16] and therefore this class of highly reduced POM cluster represents one of the most exciting developments in POM chemistry and with many potential spin-off applications in nanoscience, see Figure 2.1.

Here we start to examine the pivotal role that polyoxometalate clusters can play in the development of nanoscale devices that utilize POM components, and start to conceptualize some example systems in which POM components could have a crucial role [13, 19]. This is because such functional nanosystems can exploit the building block principle already established in this area of chemistry, coupled with the range of physical properties, and the fact that POM systems can really be seen as molecular metal oxides [20]. To demonstrate this point, a number of examples have been selected across the area of POM chemistry, including our contributions, to help highlight new directions and concepts. It should also be noted that metal oxides already play an important role in the electronics and semiconductor industry today and their solid-state properties have been studied extensively [21, 22]. Many of these concepts are not new in isolation, but the possibility of using molecular design in metal oxides to produce
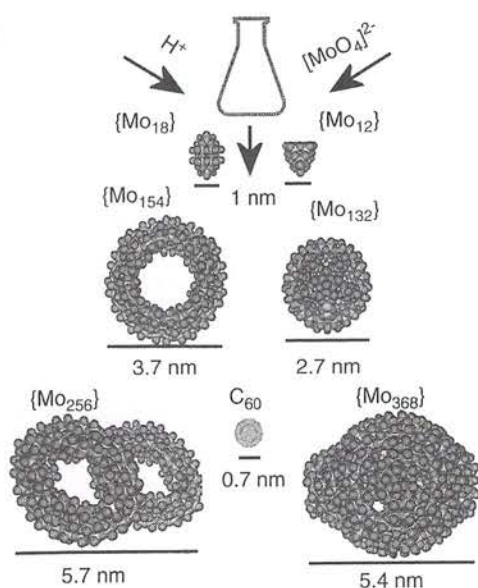
Figure 2.1 Representations of the structures of some Mo-based POM clusters (nuclearity given in subscript), all synthesized under "one-pot–one-step" acidic reaction conditions (space filling) from the well-known and studied $\{M_{12}\}/\{M_{18}\}$ Keggin/ Dawson [11, 12] ions to the $\{Mo_{154}\}$ [15]/$\{Mo_{132}\}$ [16] and $\{Mo_{256}\}$ [17]/$\{Mo_{368}\}$ [18] clusters. These clusters are compared (to scale) with C_{60} to demonstrate their macromolecular dimensions [4, 5].

functional systems that exploit size effects, ligand/hetero-ion modification, switchable properties, and cooperative electronic effects will undoubtedly be significant in the quest for functional nanosystems that start to bridge the gap between bottom-up and top-down assembly [23]. This is because POMs can be constructed that bridge large length scales and lithographic techniques (top down) could be used to direct the positioning of clusters that might be built using self-assembly (bottom up).

2.2
From POM Building Blocks to Nanoscale Superclusters

The ability to design new nanoscale systems and architectures requires access to a range of building blocks. In this respect, POM cluster chemistry can offer a large range of building blocks that are conserved between structures and it appears that they have intrinsic properties (high and variable charge and flexible ligand coordination modes) that facilitate the self-assembly of clusters containing many thousands of atoms in solution. In particular, the use of pentagonal-type

building groups directed by reduced $\{Mo^V_2\}$ units plays a key role in the synthesis of these systems and the construction of nanoscale architectures [5]. This can be taken further by considering that edge-sharing (condensed) pentagons cannot be used to tile an infinite plane, whereas exactly 12 pentagons are required, in connection with well-defined sets of hexagons, to construct spherical systems such as that observed in the truncated icosahedron – the most spherical Archimedean solid – in polyhedral viruses, or in the geodesic Fuller domes [24]. Indeed, it has been shown [15–18, 20] that the Mo-based pentagonal building blocks allow the generation of very large clusters with nuclearities between 36 and 368 metal atoms in a single cluster molecule, see Figure 2.2. These clusters can be seen to be built using a range of conserved building blocks. For instance the spherical Keplerate cluster [16] can be considered in geometrical terms to be comprised of (Pentagon)$_{12}$(Linker)$_{30}$, where Pentagon = $\{Mo(Mo)_5\}$ and Linker = $\{Mo^V_2O_4(OOR)^+\}$, $\{OMo^V(H_2O)\}^{3+}$, $\{Fe^{III}(H_2O)_2\}^{3+}$; that is, in the case of the cluster where the linkers are $\{Mo^V_2O_4(OAc)^+\}$ the overall formula is $[Mo^{VI}_{72}Mo^V_{60}O_{372}(MeCO_2)_{30}(H_2O)_{72}]^{42-}$. In the case of the $\{Mo_{256}Eu_8\} \equiv \{Mo^{VI}_{104}Mo^V_{24}Eu^{III}_4O_{388}H_{10}(H_2O)_{81}\}_2^{20-}$ system, which comprises two elliptical $\{Mo_{128}Eu_4\}$ rings, each ring is composed of 12 pentagonal units [17]. However the elliptical ring has a more complicated set of building blocks than the Keplerate cluster and is formally composed of $[\{Mo_1\}_6\{Mo_2\}_4\{Mo_8\}_2\{Mo_7\}_2\{Mo_9\}_2]$ which is similar to the building blocks found in the archetypal "big-wheel" clusters [15]. As such, the wheel clusters also incorporate a $\{Mo_2\}$ unit where the polyhedra are corner rather than edge sharing (red polyhedra in Figure 2.2). Also, the pentagonal-centered units in the $\{Mo_{132}\}/\{Mo_{368}\}$ spherical clusters are $\{Mo_6\}$ type units (central pentagonal unit with 5 octahedra attached, preserving the fivefold symmetry) whereas the pentagonal center unit in the $\{Mo_{256}\}$ and other wheel clusters has two additional $\{Mo\}$ units fused to the bottom of the $\{Mo_6\}$ to make a $\{Mo_8\}$ type unit, see Figure 2.2.
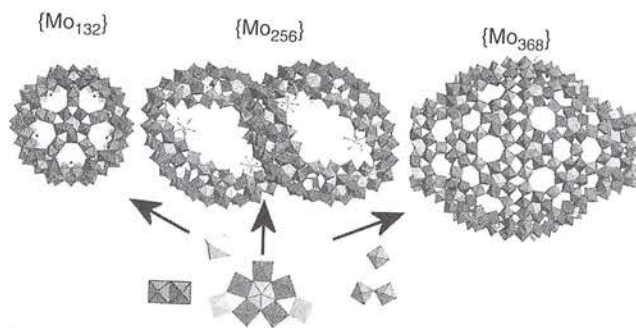
$\{Mo_{132}\}$ $\{Mo_{256}\}$ $\{Mo_{368}\}$

Figure 2.2 Structures of the $\{Mo_{132}\}^{[16]} \equiv [Mo^{VI}_{72}Mo^V_{60}O_{372}(MeCO_2)_{30}(H_2O)_{72}]^{42-}$, $\{Mo_{256}\}^{[17]} \equiv [Mo_{256}Eu_8O_{776}H_{20}(H_2O)_{162}]^{20-}$, and $\{Mo_{368}\}^{[18]} \equiv [H_xMo_{368}O_{1032}(H_2O)_{240}(SO_4)_{48}]^{48-}$, clusters shown with polyhedral plots. The structurally conserved building blocks found in these clusters is shown below; the $\{Mo_2\}$ show below on the left (edge sharing) and right hand side (corner sharing), the $\{Mo_1\}$ groups are also shown below and the central pentagonal unit of the $\{Mo_6\}$ unit is shown in light grey.

The $\{Mo_{368}\} \equiv [H_xMo_{368}O_{1032}(H_2O)_{240}(SO_4)_{48}]^{48-}$ is even more complex since it combines both negative and positive curvature [18]. The building blocks can be represented as $\{Mo(Mo_5)\}_8\{Mo(Mo_5)\}'_{32}\{Mo_2\}_{16}\{Mo_2\}'_8\{Mo_2\}''_8\{Mo_1\}_{64}$ with 40 pentagonal units being required to complete the structure and can be considered to be a hybrid between the wheel and ball clusters.

The major problem with this approach lies in establishing routes to produce reactive building blocks present in solution in significant concentrations that can be reliably utilized in the formation of larger architectures without reorganizing to other unknown fragments. Access to such building blocks has been the major limitation in stepwise growth of Mo-based POM clusters compared with the more kinetically inert W-based clusters which have shown a degree of control, as illustrated by the isolation of several W-based POMs such as the large nanoscale $\{W_{148}\}$ $\equiv [Ln_{16}As_{12}W_{148}O_{524}(H_2O)_{36}]^{76-}$ cluster [25]. Such limitations may be circumvented by adopting an approach that kinetically stabilizes the building block in solution, thereby effectively preventing its reorganization to other structure types.

In our work, while developing strategies toward this goal, we have found a new family of polyoxomolybdates [26, 27] based on the $[H_2Mo_{16}O_{52}]^{10-}$ framework which appears to achieve the first part of this goal and allows the isolation of a new structure type by virtue of the cations used to "encapsulate" this unit, thereby limiting its reorganization to a simpler structure, see Figure 2.3. Furthermore, the building block character of this anion is demonstrated when electrophilic transition metal cations M^{2+} (M = Fe, Mn, Co) are added to solutions of this cluster, resulting in $[H_2Mo_{16}M_2O_{52}]^{6-}$ species that can undergo further condensation reactions.

These clusters were trapped during the self-assembly process by bulky organic cations which appear to have restrained the clusters from reorganizing into other well-known structure types. This yields a family of POMs with a range of symmetries and nuclearities and, most importantly, the potential to really "tailor" the physical properties by changing the cluster framework. This approach relies on trapping and stabilizing nonspherical polyanions of low nuclearity and symmetry before their aggregation and rearrangement to more uniform and stable struc-
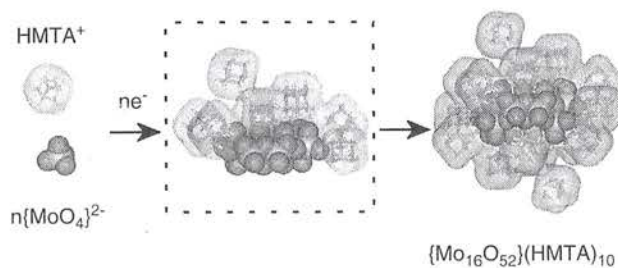

Figure 2.3 A schematic showing the "encapsulation" of the cluster units during the cluster assembly process in the presence of the bulky organo-cation HMTA (hexamethylenetetraamine).

tures. See Figure 2.4 for an example of a cluster trapped using this approach to yield a $\{Mo_{16}\} \equiv [H_2Mo_{16}O_{52}]$ [26, 27].

Furthermore, the organocations can also be used as structure-directing moieties, not only at a molecular level but also allowing the formation of polymers that enable large aggregates to assemble, see Figure 2.5 [28]. The effect of the use of encapsulating cations, here the tetra-n-butylammonium cation (n-Bu$_4$N$^+$), is demonstrated by the reaction of (n-Bu$_4$N)$_2$[Mo$_6$O$_{19}$] with silver(I) fluoride in methanol,
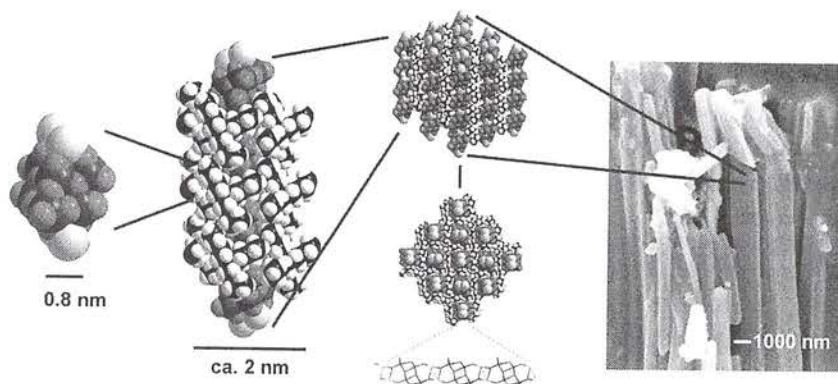
Figure 2.4 Space-filling representations of segments of the linear chain of linked [Ag^{I}Mo$^{VI}_8$O$_{26}$Ag^I]$^{2-}$ showing the growth of the structure into linear chains encapsulated by the organic n-Bu$_4$N$^+$ cations and the arrangement of the packed array of these chains, along with a stick representation of the chain framework (Mo: dark grey, O: medium grey, Ag: light grey, C: black, H: white). The organization of the packed linear chains forming microcrystals of the compound are shown on the right SEM image with the crystallographic a axis parallel to the direction of the molecular chains.
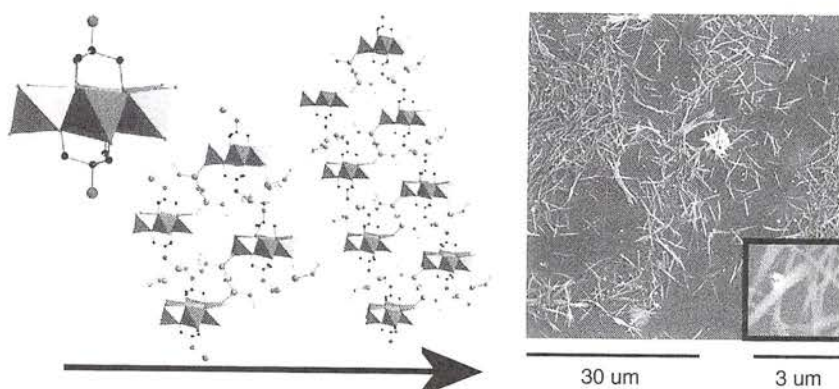

Figure 2.5 Representation of the Anderson-based, [MnMo$_6$O$_{18}$ {(OCH$_2$)$_3$CNH$_2$}$_2$]$^{3-}$, unit on the left, the network formed by complexation with {Ag$_2$(DMSO)$_4$}$^{2+}$ in the middle, and the SEM of the material on a silicon substrate.

which ultimately results in the formation of a unique one-dimensional chain structure of the composition: $(n\text{-}Bu_4N)_{2n}[Ag_2Mo_8O_{26}]_n$. Here, the flexible $n\text{-}Bu_4N^+$ cations wrap almost completely around the linear chain of linked $[Ag^IMo^{VI}_8O_{26}Ag^I]^{2-}$ units, see Figure 2.5. In the solid state these strands are packed to a network of collinear, organic "tunnels" that accommodate the polymeric $\{Ag_2Mo_8\}_\infty$ anions. The nature of the $\{Ag_2\}$ linker groups and the Ag coordination environments, however, were found to depend on the reaction conditions, which suggests that the precursors in the reaction solution are not individual $\{Ag_2\}$ and $\{Mo_8\}$ groups but, most probably, $\{Ag(Mo_8)Ag\}$-type synthons, see Figure 2.4. Silver linkers are extremely versatile in polyoxometalate chemistry simply due to the poor mismatch between the oxo and silver species.

The mismatch between the ligand preferences of Ag(I) and the Mo-based POMs can be exploited even further by using coordinative groups on the POM. For instance, by derivatizing the Anderson-type cluster via the *tris* ligand [tris(hydroxymethyl)aminomethane] which has three pendant hydroxyl groups that can replace the hydroxide groups on the surface of the Anderson cluster [29], it is possible to produce a range of materials that can be manipulated by the coordination of the Ag(I) species [30]. For instance, the Anderson derivatized with tris and complexed with Ag(I) forms a 1D chain in the solid state where the repeat unit in the chain is built from two *tris*-derived Anderson cluster $[MnMo_6O_{18}\{(OCH_2)_3CNH_2\}_2^{3-}]$ units connected via a bridging $\{Ag_2(DMSO)_4\}^{2+}$ unit and the chain is propagated by a single Ag(I) which connects to the nitrogen atom of the *tris* ligands. It is interesting that this compound, when assembled on silicon, forms a 1D wirelike structure, see Figure 2.5. This fibers observed on the surface are $>10\,\mu m$ in length with a diameter of $\sim0.5\,\mu m$. This means that the derivatized Anderson cluster appears to be a robust and useful building block with potential for the use in the self-assembly of functional materials. Given the versatile electronic properties of POMs, this building block approach might become relevant, for example, in the production of spacers of specific dimensionality for use as a skeleton for conducting interconnectors in nanoscale electronic devices, or as electron-beam resists.

It is clear that POM-based clusters have a very interesting range of accessible building blocks that bridge a number of length scales, which allows the construction of complex molecules with a great deal of flexibility and structural variation. The challenge in many POM systems is to understand and control this variation to develop the building block route even further.

2.3
From Building Blocks to Functional POM Clusters

There is little doubt that diverse physical properties common to polyoxometalates places them in an almost unmatched class of materials which could be extremely useful as hybrid materials and nanocomposites [31]. In this section we will focus on POM systems with properties that could be exploited in the development of molecular-scale devices.

2.3.1
Host–Guest Chemistry of POM-based Superclusters

The development of host–guest chemistry based on POM superstructures has been one of the most interesting developments and begins to show possibilities for POMs acting as sensors, storage capsules, and hosts that are able to respond to external stimuli. For instance molecular growth from a $\{Mo_{176}\}$ ring to a $\{Mo_{248}\}$ ring with the inner voids covered with "hub-caps" has been possible [32] as well as the complexation of a metalloporphyrin within the cavity of the $\{Mo_{176}\}$ wheel [33]. A similar assembly with a $\{W_{48}\}$ cluster has also been reported but this time including a 1st row transition metal fragment inside [34].

The Keplerate $\{Mo^{VI}_{72}Mo^{V}_{60}L_{30}\}^{n-}$ ($n = 42$ when L = acetate, $n = 72$ when L = sulfate) ball cluster provides an ideal framework to extend these ideas as it is a spherical cluster with a high charge and an accessible inner chamber with a large volume, and the nature of the surface of the inner chamber can be tuned as well as the pores. Investigations of this cluster taking up various cations such as lithium have given insight into basic principles of cation transport through "molecular pores." This was investigated using porous Keplerates with sulfate ligands on the inner surface; the cluster behaves as a semipermeable inorganic membrane open for H_2O and small cations [35]. Similar studies of the uptake/release of cations by a capsule in solution may be extended to investigate nanoscale reactions in solutions as well as a large variety of cation-transport phenomena, see Figure 2.6. The pores shown in the Keplerate have the form $\{Mo_9O_9\}$ and provide a structural motif rather similar to that of the classical crown ethers.

This comparison is even more striking for the $\{W_{36}\}$-based cluster with the formula $\{(H_2O)_4K\subset[H_{12}W_{36}O_{120}]\}^{11-}$ and includes the threefold symmetric cluster anion $[H_{12}W_{36}O_{120}]^{12-}$, see Figure 2.7. Interestingly, the cluster anion complexes a potassium ion at the center of the $\{W_{36}\}$ cluster in a $\{O_6\}$ coordination environment [36]. The $\{W_{36}\}$ structure consists of a ring of six basal W positions, an additional W position in the center of this ring, and four apical W positions in a butterfly configuration. Every W center has a distorted WO_6 octahedral coordina-
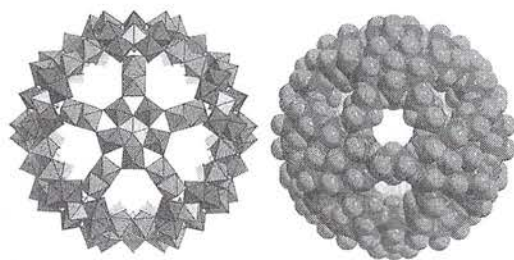

Figure 2.6 Polyhedral structure (left) and space-filling structure (right) of the $\{Mo^{VI}_{72}Mo^{V}_{60}L_{30}\}^{n-}$ ball cluster. The space-filling structure is looking directly down the one of the $\{Mo_9O_9\}$ pores.
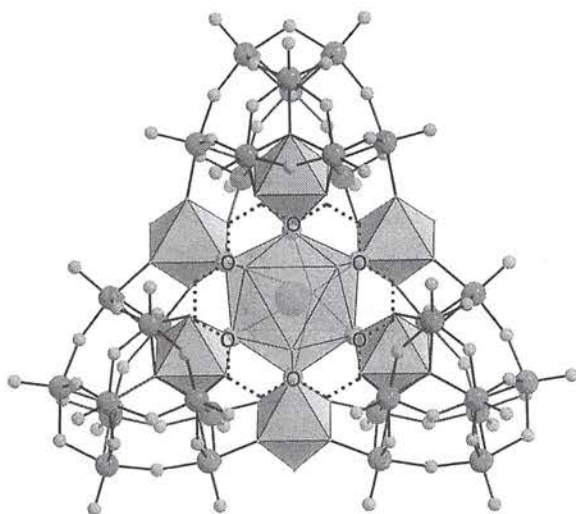
Figure 2.7 Representation on the $\{(H_2O)_4K\subset[H_{12}W_{36}O_{120}]\}^{11-}$ cluster with the central potassium ion shown behind the central polyhedra. The framework of 18-C-6 is superimposed onto the central $\{O_6\}$ moiety to scale and the six W-groups which each donate oxygen ligands to coordinate to the potassium ion are shown in polyhedral representation.

tion geometry with one terminal $W{=}O$ (W—O ~1.70 Å) extending away from the cluster; this arrangement maps extremely well onto the structure of the crown ether 18-C-6. The implications for the development of this system in a similar fashion to the crown ethers are interesting, especially the possibilities for discrimination and sensing of metal ions using this cluster framework [36].

2.3.2
Magnetic and Conducting POMs

The development of POM-based clusters incorporating paramagnetic centers is an interesting goal since it is possible to utilize existing building blocks/clusters to generate very large magnetic molecules. In fact it has been shown that it is possible to substitute the $\{Mo_2\}$ "linker" groups present in the Keplerate $\{Mo_{132}\}$, (Pentagon)$_{12}$(Linker)$_{30}$ species with Fe^{III} to yield a $\{Mo_{72}Fe_{30}\}$ cluster with the formula $[Mo_{72}Fe_{30}O_{252}(CH_3COO)_{10}\{Mo_2O_7(H_2O)\}\{H_2Mo_2O_8(H_2O)\}_3(H_2O)_{91}]$ [37]. This cluster is smaller than the parent $\{Mo_{132}\}$ structure with an outer diameter of ~25 Å and an inner diameter of ~18 Å, see Figure 2.8. Further, the $\{Mo_{72}Fe_{30}\}$ cluster comprises only Mo^{VI} atoms whereas the $\{Mo_{132}\}$ cluster contains 60 reduced Mo^V centers (the 30 linking $\{Mo_2\}$ units are reduced). The presence of the Fe(III) centers, combined with the weak antiferromagnetic exchange between these centers, means that there are 30 mainly uncorrelated spins 5/2 at room
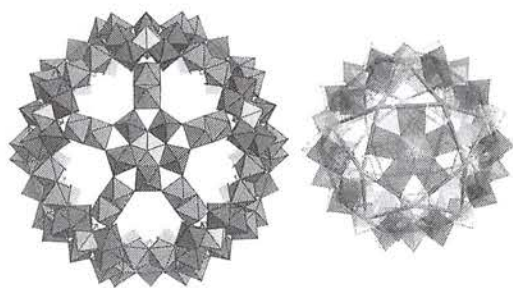
Figure 2.8 Polyhedral representations of the structures of the {Mo_{132}} (left) and {$Mo_{72}Fe_{30}$} (right) clusters to scale. The icosidodecahedron which is formed by connecting the 30 Fe centers is shown.

temperature and the cluster therefore behaves like a paramagnet with 150 unpaired electrons. The Fe(III) centers of the cluster span an icosidodecahedron and the extremely rich and interesting magnetic properties have been investigated using a simple Heisenberg model [38]. In this respect the {$Mo_{72}Fe_{30}$} has been termed a mesoscopic paramagnet for which classical behavior extends down to extraordinarily low temperatures.

The formation of hybrid materials based on POMs with stacks of partially oxidized p-electron donor molecules of tetrathiafulvalene (TTF) has been accomplished to yield conducting POM-based materials. This is interesting because the inorganic POM anion can act as a structural spacer unit, incorporate additional functionality such as a scaffold for paramagnetic ions or to act as an electron acceptor [27]. This area is progressing rapidly with the compounds based on [BEDT-TTF]$_5$[$H_3V_{10}O_{28}$] [39] and [BEDT-TTF]$_6$[Mo_8O_{26}] [40] (BEDT-TTF = bis(ethylenedithio)tetrathiafulvalene) which behave as metals down to 50 and 60 K with room temperature conductivities of 360 and 3 S cm^{-1}, respectively. In addition, a POM radical salt with metallic behavior down to 2 K has been synthesized [41]. The compound is based on [BEDOTTF]$_6$K$_2$[$BW_{12}O_{40}$] and is formed from [$BW_{12}O_{40}$]$^{5-}$ and the organic radical (BEDO-TTF) (= bis(ethylenedioxo) tetrathiafulvalene). The realization of POM-organic conducting hybrids means that devices incorporating both POM clusters and organic conductors and polymers are also accessible.

2.3.3
Thermochromic and Thermally Switchable POM Clusters

In our attempts to design functional clusters we have focused on substitution of the heteroanions within the Wells-Dawson structure to create nonconventional Dawson clusters incorporating *two* pyramidal anions. Our design rationale was based on the idea that such clusters may exhibit unprecedented properties arising from the intramolecular electronic interactions between the encapsulated anions (in this case we aimed to engineer between S···S atoms of two encapsulated sulfite ions), thus providing a novel route to manipulate the physical properties of

the $\{Mo_{18}\}$ Dawson-type clusters. The synthesis of these clusters was accomplished by extending our previous work utilizing organocations and allowed the isolation of the α-$[Mo^{VI}_{18}O_{54}(SO_3)_2]^{4-}$ (type 1) which incorporates the targeted two pyramidal sulfite SO_3^{2-} anions as the central cluster templates. This compound showed thermochromic behavior between 77 K (pale yellow) and 500 K (deep red), see Figure 2.9 [42].

In an extension of this work to W-based Dawson-like clusters we succeeded in synthesizing the analogous polyoxotungstate clusters incorporating the sulfite anion [43], $[W^{VI}_{18}O_{54}(SO_3)_2]^{4-}$ (type 1) the isostructural tungstate analog to the $\{Mo_{18}\}$ example, and $[W^{VI}_{18}O_{56}(SO_3)_2(H_2O)_2]^{8-}$ (type 2), see Figure 2.10.
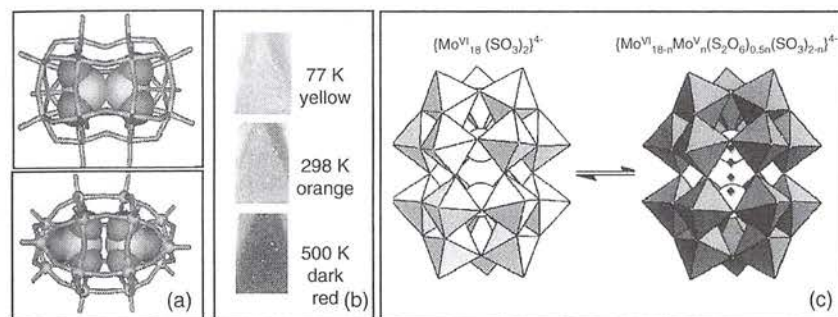

Figure 2.9 (a) The crystal structure of the new type of Sulfite-Dawson above, compared to the known sulfate-Dawson below, showing the S···S interaction. (b) are photographs of the thermochromic material at 77, 298 and 500 K. (c) Shows two polyhedral views of the low temperature sulfite-Dawson (on the left) at 77 K and the resulting high temperature sulfite-Dawson (on the right) at 500 K along with a possible mechanism for the process resulting from the formation of a partial bond between the SO_3^{2-} which would be accompanied by electron release to the cluster shell (S···S in space filling to show the interaction between the two sulfur atoms).[40]
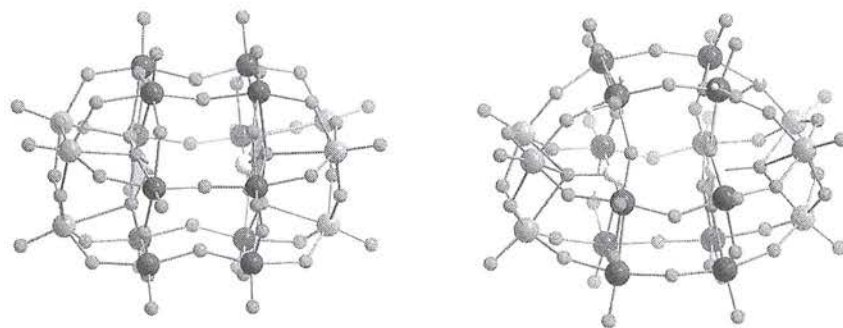

Figure 2.10 Ball-and-stick representations of the structures of the D_{3h}-symmetric α-$[W_{18}O_{54}(SO_3)_2]^{4-}$ (type 1-left) and the C_{2v}-symmetric $[W_{18}O_{56}(SO_3)_2(H_2O)_2]^{8-}$ (type 2-right) cluster anions (W: equatorial $\{W_6\}$ – dark grey, capping $\{W_3\}$ – light grey; O: small grey spheres; S: light grey sphere at the apex of the polyhedra which represent the pyramidal SO_3^{2-} units).
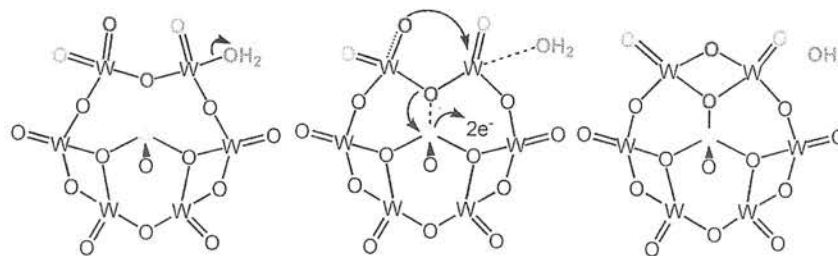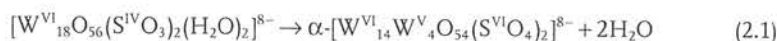
Figure 2.11 Mechanism of the internal sulfite to sulfate oxidation showing the movement of the oxygen atoms (shown faded). The equatorial cluster "belts" and the central sulfur position of a $\{W_9(SO_3)\}$ fragment is illustrated (S atoms also faded).

Comparison of the type 1 and type 2 $\{W_{18}\}$-Dawson structures shows that $[W^{VI}_{18}O_{54}(SO_3)_2]^{4-}$ also engineers the short $S\cdots S$ interaction, whereas the $[W^{VI}_{18}O_{56}(SO_3)_2(H_2O)_2]^{8-}$ cluster contains two sulfite anions that are locked into a different binding mode and appear to expand the upper part of the cage. This cluster also undergoes an interesting reaction when heated whereby a structural rearrangement allows the two embedded pyramidal sulfite ($S^{IV}O_3^{2-}$) anions to release up to four electrons to the surface of the cluster and results in the sulfate-based, deep blue, mixed-valence $[W_{18}(SO_4)_2]^{8-}$ cluster. Thus the cluster type 2 appears already surprisingly well prearranged for an internal reorganization and a concurrent internal redox reaction, in which the encapsulated sulfite anions act as embedded reducing agents and are oxidized to sulfate when heated to over 400 °C, see Figure 2.11. In the course of this reaction, a maximum of four electrons could be transferred to the metal-oxide framework, causing a color change from colorless ($\{W^{VI}_{18}\}$) to blue ($\{W^{VI}_{14}W^{V}_4\}$). The overall reaction is accompanied by the release of the two coordinated water ligands of the W centers, so the following reaction occurs:

$$[W^{VI}_{18}O_{56}(S^{IV}O_3)_2(H_2O)_2]^{8-} \rightarrow \alpha\text{-}[W^{VI}_{14}W^{V}_4O_{54}(S^{VI}O_4)_2]^{8-} + 2H_2O \qquad (2.1)$$

In this cluster system the enclosure of sulfite anions with a "correct" orientation transforms the anions from "innocent" structural templates to electronically reactive, functional units. These can now release electrons to the cluster shell upon activation by heat—the sulfite groups in type 2 clusters are "activated" whereas those in type 1 are not.

2.4
Bringing the Components Together—Towards Prototype Polyoxometalate-based Functional Nanosystems

The gap between concepts in molecular design to produce polyoxometalate integrated nanosystems or molecular-scale devices is vast due to the problem of fabrication and control of molecular orientation. Molecule-by-molecule assembly is

clearly a great challenge; therefore, the design of self-organizing and self-assembling systems utilizing ideas and inspiration from supramolecular chemistry to form functional molecular systems that can be connected from the molecule to the macroscale world is highly desirable [44]. However, the route to achieve such a grand aim is still unclear and many scientific fields are converging on the development of nanoscale and molecular electronics and interdisciplinary approaches are being developed to address the significant scientific and technical barriers. Clearly the design and synthetic approaches to polyoxometalates, and the fact these clusters can be constructed over multiple length scales, along with their almost unmatched range of physical properties means that they are great candidates to be used as both the scaffold and the functional part of any nanodevice. There is therefore great scope to investigate the self-assembly of functional POM systems on surfaces and in the crystalline state to produce architectures that can be fabricated to form a polyoxometalate-based device. Indeed, recent work in the production of thin films of polyoxometalate clusters [45], and the use of POM clusters in "nanocasting" [46] are examples where the cross-disciplinary approach is beginning to utilize the potential of this class of clusters. One possible approach to the fabrication of POM may, for instance, utilize lithographic techniques to prepare patterned substrates for the formation of "functional" polyoxometalate clusters, or even utilize the POM cluster in the growth of nanoscale connects that can be directed to individual electrodes patterned using lithography [47].

In one such approach we seek to exploit the potential signal transduction properties of the thermochromic Dawson [40] polyoxometalates and combine this with a fluorescent POM-hybrid to produce a device that could respond optically as a function of the local environment, see Figure 2.12. In this example, the clusters would be positioned on a gold surface using SAMs (Self-assembled monolayer) with a cationic tail and local positional control could be aimed using self-assembly, or even by means of an atomic force microscope tip.

The challenge now is to design individual POM cluster molecules that can interact both with each other and with the macroscale (as shown in Figure 2.12), in a desired fashion in response to inputs and environmental effects, so that a functioning molecular system is really constructed.
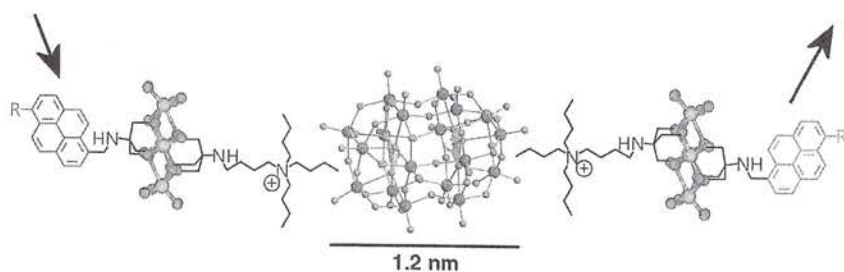

1.2 nm

Figure 2.12 Schematic of a surface assembly of a pyrene-derivatized Anderson (left) that absorbs in the blue arranged next to a $[Mo^{VI}_{18}O_{54}(SO_3)_2]^{4-}$ cluster species which has thermochromic properties. On the right there is a pyrene-derivatized Anderson cluster hybrid that fluoresces. The aim is to use the thermochromic {Mo_{18}}, which is positioned between the two pyrene-Anderson units, to control the response of the system to light.

2.5
Acknowledgments

References

1 Badjic, J.D., Balzani, V., Credi, A., Silvi, S. and Stoddart, J.F. (2004) *Science*, 303, 1845.

2 Collier, C.P., Wong, E.W., Belohradský, M., Raymo, F.M., Stoddart, J.F., Kuekes, P.J., Williams, R.S. and Heath, J.R. (1999) *Science*, 285, 391–4.

3 Yoshimura, I., Miyahara, Y., Kasagi, N., Yamane, H., Ojida, A. and Hamachi, I. (2004) *Journal of the American Chemical Society*, 126, 12204–5. Maue, M. and Schrader, T. (2005) *Angewandte Chemie (International Ed. in English)*, 44, 2265–70.

4 Long, D.-L., Burkholder, E. and Cronin, L. (2007) *Chemical Society Reviews*, 36, 105–21.

5 Cronin, L. (2002) The potential of pentagonal building blocks, in *Inorganic Chemistry Highlights* (eds G. Meyer, D. Naumann and L. Wesemann), Wiley-VCH Verlag GmbH, Weinheim, pp. 113–21.

6 Neumann, R. and Dahan, M. (1997) *Nature*, 388, 353–5. Mizuno, N. and Misono, M. (1998) *Chemical Reviews*, 98, 199–218.

7 Katsoulis, D.E. (1998) *Chemical Reviews*, 98, 359–87. Yamase, T. (1998) *Chemical Reviews*, 98, 307–25.

8 Rüther, T., Hultgren, V.M., Timko, B.P., Bond, A.M., Jackson, W.R. and Wedd, A.G. (2003) *Journal of the American Chemical Society*, 125, 10133–43.

9 Anderson, T.M., Neiwert, W.A., Kirk, M.L., Piccoli, P.M.B., Schultz, A.J., Koetzle, T.F., Musaev, D.G., Morokuma, K., Cao, R. and Hill, C.L. (2004) *Science*, 306, 2074–7.

10 Müller, A., Das, S.K., Talismanov, S., Roy, S., Beckmann, E., Bögge, H., Schmidtmann, M., Merca, A., Berkle, A.,

Allouche, L., Zhou, Y. and Zhang, L. (2003) *Angewandte Chemie (International Ed. in English)*, 42, 5039–44.

11 Pope, M.T. (1987) Isopolyanions and Heteropolyanions, in *Comprehensive Coordination Chemistry*, (eds G. Wilkinson, R.D. Gillard and J.A. McCleverty), Pergamon Press, Vol. 3, pp. 1023–58.

12 Cronin, L. (2004) High nuclearity polyoxometalate clusters, in *Comprehensive Coordination* (eds I.J.A. McCleverty and T.J. Meyer), Elsevier, Amsterdam, Vol. 7, pp. 1–57.

13 Long, D.L. and Cronin, L. (2006) *Chemistry–A European Journal*, 12, 3698.

14 Scheele, W. (1971) *Sämtliche Physische und Chemische Werke*. (ed. D.S.F. Hermbstädt) M. Sändig oHG, Niederwalluf/Wiesbaden, Vol. 1, pp. 185–200 (reprint, original 1783).

15 Müller, A., Krickemeyer, E., Meyer, J., Bögge, H., Peters, F., Plass, W., Diemann, E., Dillinger, S., Nonnenbruch, F., Randerath, M. and Menke, C. (1995) *Angewandte Chemie (International Ed. in English)*, 34, 2122–4.

16 Müller, A., Krickemeyer, E., Bögge, H., Schmidtmann, M. and Peters, F. (1998) *Angewandte Chemie (International Ed. in English)*, 37, 3360. Müller, A., Krickemeyer, E., Bögge, H., Schmidtmann, M. and Peters, F. (1998) *Angewandte Chemie (International Ed. in English)*, 37, 3359–63.

17 Cronin, L., Beugholt, C., Krickemeyer, E., Schmidtmann, M., Bögge, H., Koegerler, P., Luong, T.K.K. and Müller, A. (2002) *Angewandte Chemie (International Ed. in English)*, 41, 2805–8.

18 Müller, A., Beckmann, E., Bögge, H., Schmidtmann, M. and Dress, A. (2002) *Angewandte Chemie (International Ed. in English)*, 41, 1162–7.

19 Kögerler, P. and Cronin, L. (2005) *Angewandte Chemie (International Ed. in English)*, 44, 844–5.

20 Pope, M.T. and Müller, A. (eds) (1994) *Polyoxometalates. From Platonic Solids to Anti-retroviral Activity*, Kluwer Academic Publishers, Dordrecht, The Netherlands.

21 Maekawa, S., Tohyama, T., Barnes, S.E., Ishihara, S., Koshibae, W. and Khaliullin, G. (2004) *Physics of Transition Metal Oxides*, Springer, Berlin, pp. 1–137.

22 Cox, P.A. (1992) *Transition Metal Oxides: An Introduction to Their Electronic Structure and Properties*, Clarendon press, Oxford.

23 Lehn, J.M. (2002) *Proceedings of the National Academy of Sciences of the United States of America*, 99, 4763–8.

24 Kroto, H.W., Heath, J.R., O'Brien, S.C., Curl, R.F. and Smalley, R.E. (1985) *Nature*, 318, 162–3.

25 Wassermann, K., Dickman, M.H. and Pope, M.T. (1997) *Angewandte Chemie (International Ed. in English)*, 36, 1445–8.

26 Long, D., Kögerler, P., Farrugia, L.J. and Cronin, L. (2003) *Angewandte Chemie (International Ed. in English)*, 42, pp. 4180–3.

27 Long, D.L., Kögerler, P., Farrugia, L.J. and Cronin, L. (2005) *Dalton Transactions (Cambridge, England: 2003)*, 1372–80.

28 Abbas, H., Pickering, A.L., Long, D.-L., Kögerler, P. and Cronin, L. (2005) *Chemistry – A European Journal*, 11, 1071–8.

29 Favette, S., Hasenknopf, B., Vaissermann, J., Gouzerh, P. and Roux, C. (2003) *Chemical Communications*, 2664–5.

30 Song, Y.-F., Abbas, H., Ritchie, C., McMillian, N., Long, D.-L., Gadegaard, N. and Cronin, L. (2007) *Journal of Materials Chemistry*, DOI: 10.1039/b617830h.

31 Yamase, T. and Pope, M.T. (eds) (2002) *See in Polyoxometalate Chemistry for Nano-Composite Design*, Kluwer, New York.

32 Müller, A., Shah, S.Q.N., Bögge, H. and Schmidtmann, M. (1999) *Nature*, 397, 48–50.

33 Tsuda, A., Hirahara, E., Kim, Y.-S., Tanaka, H., Kawai, T. and Aida, T. (2004) *Angewandte Chemie (International Ed. in English)*, 43, 6327–31.

34 Mal, S.S. and Kortz, U. (2005) *Angewandte Chemie (International Ed. in English)*, 44, 3777–80.

35 Müller, A., Rehder, D., Haupt, E.T.K., Merca, A., Bögge, H., Schmidtmann, M. and Heinze-Brückner, G. (2004) *Angewandte Chemie (International Ed. in English)*, 43, 4466–70.

36 Long, D.-L., Abbas, H., Kögerler, P. and Cronin, L. (2004) *Journal of the American Chemical Society*, 126, 13880–1.

37 Müller, A., Sarkar, S., Shah, S.Q.N., Bögge, H., Schmidtmann, M., Sarkar, S., Kögerler, P., Hauptfleisch, B., Trautwein, A.X. and Schünemann, V. (1999) *Angewandte Chemie (International Ed. in English)*, 38, 3238–41.

38 Müller, A., Luban, M., Schröder, C., Modler, R., Kögerler, P., Axenovich, M., Schnack, J., Canfield, P., Bud'ko, S. and Harrison, N. (2001) *Chemphyschem: A European Journal of Chemical Physics and Physical Chemistry*, 2, 517–21.

39 Coronado, E., Galán-Mascarós, J.R., Giménez-Saiz, C., Gómez-García, C.J., Martínez-Ferrero, E., Almeida, M. and Lopes, E.B. (2004) *Advanced Materials (Deerfield Beach, Fla.)*, 16, 324–7.

40 Lapinski, A., Starodub, V., Golub, M., Kravchenko, A., Baumer, V., Faulques, E. and Graja, A. (2003) *Synthetic Metals*, 138, 483–9.

41 Coronado, E., Giménez-Saiz, C., Gómez-García, C.J. and Capelli, S.C. (2004) *Angewandte Chemie (International Ed. in English)*, 43, 3022–5.

42 Long, D.L., Kögerler, P. and Cronin, L. (2004) *Angewandte Chemie (International Ed. in English)*, 43, 1817–20. Baffert, C., Boas, J.F., Bond, A.M., -L. Long, P., Kögerler D., Pilbrow, J.R. and Cronin, L. (2006) *Chemistry – A European Journal*, 12, 8472–83.

43 Long, D.-L., Abbas, H., Kögerler, P. and Cronin, L. (2005) *Angewandte Chemie (International Ed. in English)*, 44, 3415–9.

44 Nakamura, T., Matsumoto, T., Tada, H. and Sugiura, K.-I. (eds) (2003) *Chemistry of Nanomolecular Systems: Towards the*

Realization of Nanomolecular Devices,
Springer Series in Chemical Physics 70,
Springer-Verlag, New York.

45 Liu, S., Kurth, D.G., Möhwald, H. and
Volkmer, D. (2002) *Advanced Materials
(Deerfield Beach, Fla.),* **14**, 225–8.

46 Polarz, S., Smarsly, B., Göltner, C. and
Antonietti, M. (2000) *Advanced Materials
(Deerfield Beach, Fla.),* **12**, 1503–7.

47 Song, Y., Long, D.-L. and Cronin, L. (2007)
*Angewandte Chemie (International Ed. in
English),* **46**, 1340–4.